THE INFLUENCE OF THE SST TURBULENCE MODEL COEFFICIENTS ON DETERMINING THE SHOCK WAVE POSITION OF A TRANSONIC FLOW OVER AN AIRFOIL

Paulo Arthur Beck, 00080322@ufrgs.br
Horacio Antônio Vielmo, vielmoh@mecanica.ufrgs.br
Department of Mechanical Engineering, Federal University of Rio Grande do Sul (UFRGS),
Rua Sarmento Leite 425, 90050-170, Porto Alegre, RS, Brazil.

Abstract. *This paper presents a numerical analysis on the influence of the SST turbulence model's diffusion coefficients in determining the position of the shock wave due to a transonic flow over the OAT15A airfoil. The conservation equations for mass and momentum, the turbulence model's equations for the turbulent kinetic energy and the specific dissipation rate, the enthalpy and the internal energy equations modeled the flows. The Finite Volume Method, as implemented by the commercial software Star-CCM+, approximated the flows to a discrete computational domain of O-mesh topology and hexahedral volumes, generating a system equations solved using a coupled approach. A mesh independency study verified the computation accuracy. The numerical results referenced experimental data found in literature in order to validate the numerical results. The shock wave location, the drag coefficient and the lift coefficient have been computed with greater accuracy by choosing values for the turbulence model diffusion coefficients that are realizable and yet constrained to values which produce correct near wall solution.*

Keywords*: SST Turbulence Model, Finite Volume Method, Shock Wave Position, OAT15A, Star-CCM+*

1. INTRODUCTION

This paper presents a numerical analysis on the influence of the SST turbulence model's diffusion coefficients in determining the position of the shock wave due to a transonic flow over an airfoil.

The interaction between the shock wave and the boundary layer causes the flow to separate and such interaction is highly sensitive to the boundary-layer turbulence state and its response to the deceleration caused by the shock wave (Bigarella and Azevedo, 2007). The freestream conditions and the eddy viscosity levels at the boundary-layer edge influence that state and therefore the skin friction coefficient. That in turn determines the size of the separation bubble and the shock location. Kok (2000) suggested constraints to be applied in the k-ω turbulence model variants when setting the diffusion coefficients in order to eliminate the freestream dependency while maintaining the correct near wall solution. In this work, those constraints are applied in the SST turbulence model as implemented by the commercial software Star-CCM+. The numerical results are validated against experimental data from case A11 of the AGARD-AR-303 report (Rodde and Archambaud, 1994). That case corresponds to highly accurate wind tunnel measurements of transonic flows over the OAT15A transonic airfoil.

2. FORMULATION

The Navier-Stokes equations in Cartesian integral form for an arbitrary control volume V with differential surface area $\mathbf{da}$ is

$$\frac{d}{dt}\left[\int_V \mathbf{W}dV + \oint (\mathbf{F}-\mathbf{G})\cdot\mathbf{da}\right] = \int_V \mathbf{H}dV, \tag{1}$$

where **W, F, G** and **H** are column vectors holding the conserved quantities, the inviscid terms, the viscous terms and the resultant **f** of the body forces respectively. In Eq. (1),

$$\mathbf{W}=\begin{bmatrix}\rho\\ \rho v\\ \rho E\end{bmatrix}, \mathbf{F}=\begin{bmatrix}\rho\mathbf{v}\\ \rho\mathbf{v}\otimes\mathbf{v}+p\mathbf{I}\\ \rho\mathbf{v}H\end{bmatrix}, \mathbf{G}=\begin{bmatrix}0\\ \mathbf{T}\\ \mathbf{T}\cdot\mathbf{v}\end{bmatrix}, \mathbf{H}=\begin{bmatrix}0\\ \mathbf{f}\\ 0\end{bmatrix} \tag{2}$$

and ρ, **v**, E, and p are the density, velocity, total energy per unit mass, and pressure of the fluid, respectively. **I** is the identity tensor and the total energy E relates to the total enthalpy H by $E = H - p/\rho$ where $H = h + |\mathbf{v}|^2/2$ and $h = C_p\mathrm{T}$. For a mean flow with a turbulent viscosity, the Boussinesq approximation models the viscous stress tensor **T** such that

$$\mathbf{T} = (\mu + \mu_t)\left[\nabla\mathbf{v} + \nabla\mathbf{v}^{\mathrm{T}} - \frac{2}{3}(\nabla\cdot\mathbf{v})\mathbf{I}\right]. \tag{3}$$

In Eq. (3), μ is the dynamic viscosity and μ_t is the turbulent viscosity. To evaluate the later, the SST turbulence model (Menter, 1993) is used. The transport equations for the SST model are:

$$\frac{d}{dt}\int_V \rho k dV + \oint_A \rho k\mathbf{v}\cdot\mathbf{da} = \oint_A (\mu + \sigma_k\mu_t)\nabla k\cdot\mathbf{da} + \int_V \left(G_k - \rho\beta^* f_{\beta^*}(\omega k - \omega_0 k_0) + S_k\right)dV\,, \tag{4}$$

$$\frac{d}{dt}\int_V \rho\omega dV + \oint_A \rho\omega\mathbf{v}\cdot\mathbf{da} = \oint_A (\mu + \sigma_\omega\mu_t)\nabla\omega\cdot\mathbf{da} + \int_V (G_\omega - \rho\beta f_\beta(\omega^2 - {\omega_0}^2) + D_\omega + S_\omega)dV. \tag{5}$$

In the equations above, k is the turbulence kinetic energy, ω is the turbulence specific dissipation rate, S_k and S_ω are specified source terms, k_0 and ω_0 are the ambient turbulence values in source terms that counteract turbulence decay, σ_ω, σ_k, β and β^* are model coefficients. The function f_β is a vortex-stretching modification designed to overcome the round-jet/plane jet anomaly and the f_{β^*} function ameliorates the dependence of the model on free-stream boundary conditions (Wilcox, 1998). Equation (6) gives the turbulence production term G_k :

$$G_k = \mu_t S^2 - \frac{2}{3}\rho k\nabla\cdot\mathbf{v} - \frac{2}{3}\mu_t(\nabla\cdot\mathbf{v})^2. \tag{6}$$

The production of ω evaluates as

$$G_\omega = \rho\gamma\left[(S^2 - \frac{2}{3}(\nabla\cdot\mathbf{v})^2) - \frac{2}{3}\omega\nabla\cdot\mathbf{v}\right], \tag{7}$$

where γ is a blended coefficient of the model and $S = |\mathbf{S}| = \sqrt{2\mathbf{S}\colon\mathbf{S}^{\mathrm{T}}}$ is the modulus of the mean strain rate tensor $\mathbf{S} = 1/2\,(\nabla\mathbf{v} + \nabla\mathbf{v}^{\mathrm{T}})$. The term D_ω is a cross-derivative term given by Eq. (8):

$$D_\omega = (1 - F_1)\rho 2\sigma_{\omega 2}\frac{1}{\omega}\nabla k\cdot\nabla\omega. \tag{8}$$

In the above equation, F_1 is a blending function and $\sigma_{\omega 2}$ is a model coefficient. The turbulent viscosity computes as

$$\mu_t = \rho k T, \tag{9}$$

where T is the turbulent time scale evaluated using the realizability constraint as proposed by Durbin (1996), Eq. (10):

$$T = \min\left(\frac{1}{\max(\frac{\omega}{\alpha^*}, (SF_2)/a_1}, \frac{C_T}{\sqrt{3}S}\right). \tag{10}$$

The realizable time scale coefficient C_T has a default value of 0.6 and

$$F_2 = \tanh(arg_2^2), \tag{11}$$

$$\mathrm{arg}_2 = \max\left(\frac{2\sqrt{k}}{\beta^*\omega y}, \frac{500\mu}{\rho y^2\omega}\right). \tag{12}$$

The coefficient a_1 has the value 0.31. The coefficients in the model are calculated from the blending function F_1such that each coefficient ∅ is given by

$$\emptyset = F_1\emptyset_1 + (1 - F_1)\emptyset_2. \tag{13}$$

The coefficients of Set 1 ($\emptyset_1$) are

$$\beta_1 = 0.0750, \sigma_{k1} = 0.85, \sigma_{\omega 1} = 0.5, \kappa = 0.41, \gamma_1 = \frac{\beta_1}{\beta^*} - \sigma_{\omega 1}\frac{\kappa^2}{\sqrt{\beta^*}}. \quad (14)$$

The coefficients of Set 2 ($\emptyset_2$) are

$$\beta_2 = 0.0828, \sigma_{k2} = 1.0, \sigma_{\omega 2} = 0.856, \kappa = 0.41, \gamma_2 = \frac{\beta_2}{\beta^*} - \sigma_{\omega 2}\frac{\kappa^2}{\sqrt{\beta^*}}. \quad (15)$$

The blending function F_1 evaluates by Eq. (16),

$$F_1 = \tanh(arg_1^4). \quad (16)$$

In the preceding equation,

$$\arg_1 = \min(\max\left(\frac{\sqrt{k}}{0.09\omega y}, \frac{500\mu}{\rho y^2 \omega}\right), \frac{2k}{y^2 CD_{k\omega}}) \quad (17)$$

and y is the distance to the nearest wall. The $CD_{k\omega}$ term evaluates by Eq. (18),

$$CD_{k\omega} = \max\left(\frac{1}{\omega}\nabla k \cdot \nabla\omega, 10^{-20}\right). \quad (18)$$

Since this numerical analysis models a compressible flow, the turbulence model's compressibility correction is enabled to account for dilatation dissipation. Such correction is achieved by replacing the coefficient β^* by β_c^*, Eq. (19):

$$\beta_c^* = \beta^*[1 + \xi^* F(M_t)]. \quad (19)$$

Similarly, the coefficient β computed from the blending equation of Eq. (13) is replaced by the value given by Eq. (20),

$$\beta_c = \beta - \beta^* \xi^* F(M_t). \quad (20)$$

The value of the coefficient ξ^* is 1.5 and the compressibility function is defined as $F(M_t) = [M_t^2 - M_{t0}^2]H(M_t - M_{t0})$, where $M_{t0}^2 = 0.25$ and M_t^2 is the turbulence Mach number, defined by $M_t^2 = 2k/a^2$, a being the speed of sound. $H(x)$ denotes the Heaviside step function.

3. MODEL

The physical model is ONERA's OAT15A transonic airfoil, a 12.3% thick supercritical airfoil for transport aircraft. The design point of the airfoil is $M_\infty = 0.73$ and $C_L = 0.65$. The main feature of the flow over that airfoil is an interaction between the boundary-layer and the shock wave. In order to validate the numerical results in this work, the experimental data from case A11 of the AGARD-AR-303 report (Rodde and Archambaud, 1994) has been selected. That case corresponds to measurements of the drag, lift and pressure coefficients for an OAT15A airfoil with chord c = 0.15 m at 1.15º angle of attack. Table 1 presents the freestream conditions for that case.

Table 1 - Freestream conditions of the Case A11.

P_∞ (Pa)	T_∞ (K)	ρ_∞ (kg/m^3)	μ_∞ (Pa · s)	a_∞ (m/s)	M_∞	U_∞ (m/s)	Re	Turbulence Intensity	μ_t/μ
101325	300	1.1772	1.85E-05	347.12	0.724	251.32	2.39E+06	1.00E-2	10

The numerical model approximates the airfoil's profile with 406 points in both upper and lower sides and 55 points in the trailing edge. The computational domain stretches outwards from the airfoil's profile up to approximately 300 chords in any surface normal direction, thus having "O-Mesh" topology. The domain's span is sized as 10% of the airfoil's chord and symmetry planes delimit it. Adiabatic, non-slip, non-permeable walls and a freestream boundary, set with the values in Tab. 1, complete the boundary types.

Hexahedral volumes discretize the computational domain. The boundary-layer design aims to achieve wall $y^+ \cong 1$. Figure 1 pictures a cross-section of the computational domain near the airfoil surfaces. The darker areas represent the boundary-layer region and the node clustering at the leading and trailing edges.

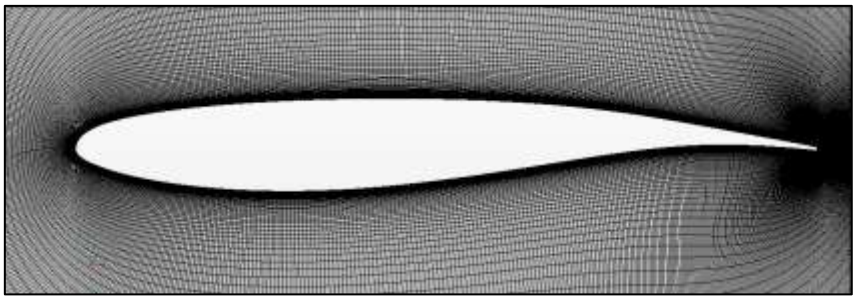

Figure 1 - The computational domain near the airfoil surfaces.

4. NUMERICAL METHODOLOGY

The Finite Volume Method implemented by the software Star-CCM+ (CD-adapco, 2012) is used to subdivide the computational domain into a finite number of control volumes corresponding to the mesh volumes. The conservation equations for mass, momentum and energy are simultaneously solved using a pseudo-time marching approach for the steady estate. The spatial integration is implicit, coupled with an algebraic multi-grid method. The discretization scheme for evaluating face values for convection and diffusion fluxes is the second-order upwind. The Courant number is set to 5.

The mesh independency has been verified by evaluating the grid convergence index (CGI) devised by Roache (1998). This index, based on the generalized Richardson extrapolation, provides a measure of the computation's accuracy. For a numerical method that is accurate to order *p* (theoretically 2 for the Finite Volume Method), the GCI for a given flow property *f* is

$$\mathrm{GCI} = 1.25\frac{|\varepsilon_h|}{r^p - 1},\ \varepsilon_h = \frac{f_{fine} - f_{coarse}}{f_{fine}}. \tag{21}$$

In Eq. (21), *r* is the ratio of fine-grid to coarse-grid dimension. The finest grid corresponds to 406 nodes in both upper and lower surfaces of the airfoil, 55 nodes in the trailing edge, 3 nodes span wise and 152 nodes in any surface normal direction, totaling 260928 mesh volumes. Taking the flow property f as being the drag coefficient c_d, the authors obtained CGI $\cong$ 1.2 % for the finest grid, used in all simulations.

5. RESULTS AND DISCUSSION

In order to analyze the effect on the shock location by changing the values of the turbulence model's diffusion coefficients, the default values of the SST turbulence model in Eq. (15) have been used to create a baseline case for comparisons. For that case, the drag coefficient is c_d = 114.9 drag counts (one drag count equals 1E-4) and c_l = 0.69.

Figure 2a presents a plot of the "BASELINE" distribution of the pressure coefficient c_p over the airfoil's upper and lower surfaces, superposed with the experimental data ("ONERA CASE 11") where c_d = 106.0 drag counts and c_l = 0.59. Figure 2b pictures a plot of the baseline skin friction coefficient c_f distribution over the airfoil's upper surface. In all plots, the numerical data is taken at the model's middle cross-section. In Fig. 2a, the sharp increase in c_p at $x \cong 0.06$ m is due to the shock wave formation. In Fig. 2b, the drop in c_f is initially due to turbulence transition and then to the shock wave, located at x = 0.059016 m.

In "CASE-01", the authors investigated the effect of the diffusion coefficients on the shock location. According to Kok (2000), the dependence on the freestream values for the *k*-ω turbulence model variants, like the SST, can be effectively eliminated by setting constraints to the values the diffusion coefficients assume. Those constraints are:

$$\sigma_{\omega 2} - \sigma_{k2} + \sigma_d > 0, \tag{22}$$

$$\sigma_{k2} - \sigma_d > 0, \tag{23}$$

$$\sigma_{\omega 2} - \sigma_{k2} + \sigma_d \leq \sigma_{k2}\sigma_{\omega 2}. \tag{24}$$

In the preceding equations, σ_d corresponds to the $2\sigma_{\omega 2}$ term in Eq. (8). For the SST model, $\sigma_{k2} = 1$ and $\sigma_{\omega 2} = 0.856$ per Eq. (15). Those coefficients satisfy the constraint imposed by Eq. (22), but fail for equations (23) and (24). The following choice of values for σ_{k2} and $\sigma_{\omega 2}$ satisfies all formulated constraints and is applied in "CASE-01":

$$\sigma_{k2} = 1.722, \sigma_{\omega 2} = 0.856. \tag{25}$$

Figure 3 plots the distribution of the pressure and skin friction coefficients for that case. An upstream shift in the shock location is observed in Figures 3a and 3b, the new position corresponding to x = 0.056438 m. That shift is attributable to the drop in the skin friction coefficient, causing the separation bubble to move forward and thus dislocating the shock location upstream the flow. The drag coefficient for CASE-01 is c_d = 110.4 drag counts and c_l = 0.67, values in closer agreement to the experimental case.

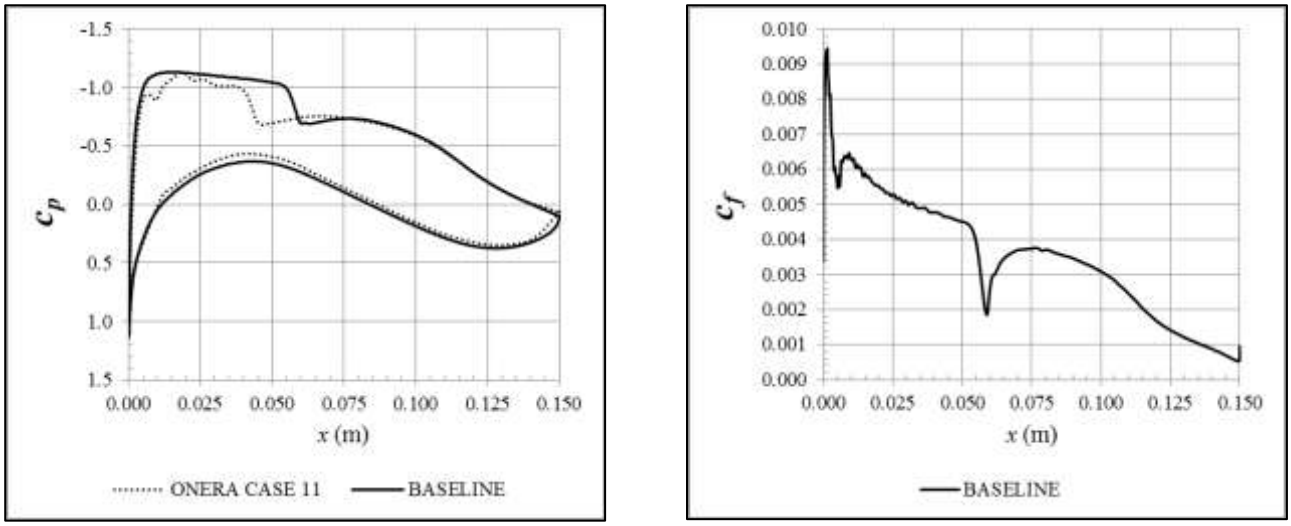

a b

Figure 2 – Distribution of the pressure coefficient (a) and the skin friction coefficient (b), BASELINE case.

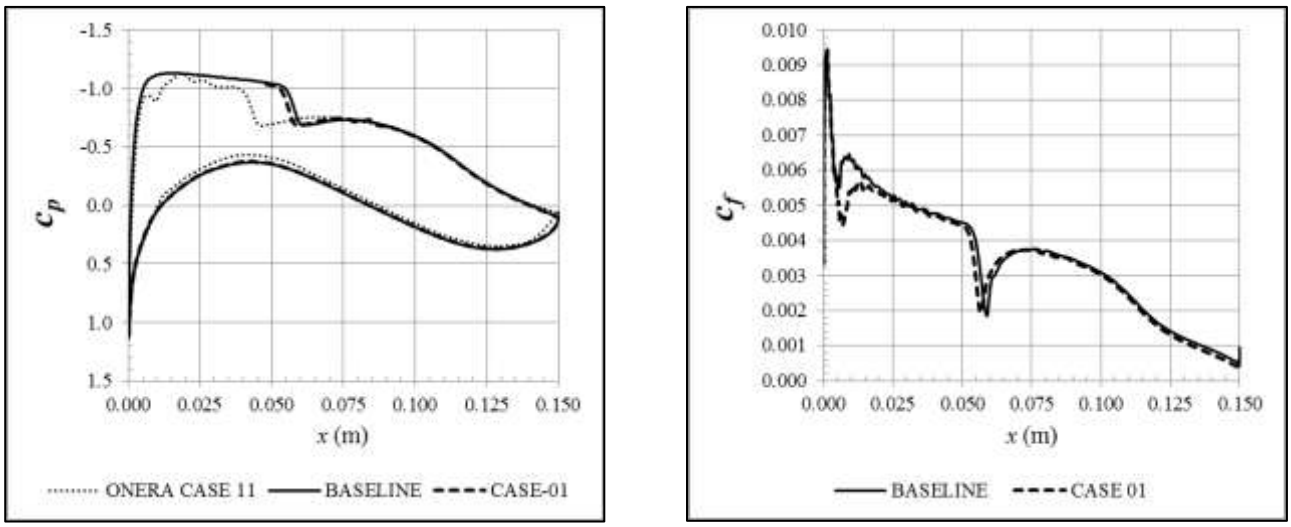

a b

Figure 3 – Distribution of the pressure coefficient (a) and the skin friction coefficient (b), CASE-01.

6. CONCLUSIONS

This paper presented an analysis on the influence of the SST turbulence model's diffusion coefficients in determining the position of the shock wave due to a transonic flow over the OAT15A airfoil. The experimental data from case A11 of the AGARD-AR-303 report has been selected to validate the numerical results. The conservation equations for mass and momentum, the turbulence model's equations for the turbulent kinetic energy and the specific dissipation rate, the enthalpy and the internal energy equations modeled the flows. The Finite Volume Method, as implemented by the commercial software Star-CCM+, approximated the model to a discrete computational domain of O-mesh topology and hexahedral volumes, generating a system equations solved using a coupled approach. The mesh independency study verified the computation results. By choosing values for the diffusion coefficients that are realizable and yet constrained to values which produce correct near wall solution, the shock wave location, the drag coefficient and the lift coefficient have been computed with greater accuracy and in closer agreement with the experimental data.

7. ACKNOWLEDGMENTS

The authors thank CNPq and CAPES (P.A. Beck graduate scholarship) for the financial support.

8. REFERENCES

Bigarella, E.D. V, Azevedo, J.L.F., 2007. "Advanced Eddy-Viscosity and Reynolds-Stress Turbulence Model Simulations of Aerospace Applications", AIAA Journal, Vol. 45, No.10.

CD-adapco, 2012. User Guide Star-CCM+ Version 7.04.01, pp. 4886-4895.

Durbin, P.A., 1996. "On the k-ε stagnation point anomaly", Int. J. Heat and Fluid Flow, Vol. 17, pp. 89-90.

Kok, J.C., 2000. "Resolving the Dependence on Freestream Values for the *k*-ω Turbulence Model", AIAA Journal, Vol. 38, No. 7, pp. 1292-1295.

Menter, F.R., 1993. "Zonal Two-Equation k-Omega Turbulence Models for Aerodynamic Flows", AIAA Paper 93-2906, July 1993.

Roache, P.J., 1998. Verification and Validation in Computational Science and Engineering, Hermosa Publishers, Albuquerque, New Mexico, USA. pp. 107-207.

Rodde, A.M., Archambaud, J.P., 1994. OAT15A Airfoil Data, A selection of Experimental Test Cases for the Validation of CFD Codes, NATO AGARD, No. AGARD-AR-303, Case A-11.

Wilcox, D.C., 1998. Turbulence Model for CFD, 2nd ed., DCW Industries, Inc., La Cañada, CA, 1998, pp. 119-122.